III. 臨床応用の進歩

眼科角膜領域再生医療

辻川元一　西田幸二

Regenerative medicine in cornea

Motokazu Tsujikawa, Kohji Nishida
Department of Ophthalmology, Osaka University Graduate School of Medicine

Abstract

Cornea is unique organ in its transparency. It consists of three different layers epithelium, stroma, and endothelium. Defect of each layers decrease the transparency resulting in blindness. Corneal transplant from donors is performed for these conditions. However it sometimes does not work because of immuno-rejection and shortage of donors is still problem. Regenerative medicine resolves these problems. According to epithelium, we had succeeded in making epithelial sheet from oral mucosa epithelium. The sheet is clear and very resembles normal corneal epithelium in histology. We have auto transplantation of this epithelial sheet to severe corneal deficiency patients and obtained good clinical results. According to endothelium, we are trying to make the sheet from various stem sells including iPS cells.

Key words: regenerative medicine, cornea, epithelium, endothelium

はじめに

角膜は光感覚器受容体である眼の光学的特性を担うため，透明で強固なドーム上の組織である．角膜上皮，角膜実質，角膜内皮の3層からなり，その機能上血管をもたない無血管組織である．疾患，外傷などでその透明性が損なわれた場合，ドナー角膜を用いた角膜移植法が実施されている．現在の角膜移植は献眼に依存しているが，我が国における提供数は絶対的に少なく，多くの患者が移植を待っている状態である．更に，後述するようにStevens-Johnson症候群などの重篤な角結膜疾患では，拒絶反応などのため他家移植の術後成績は良好ではない．これらのドナー不足および拒絶反応の問題を解決する手段として，患者自身の幹細胞・前駆細胞を用いた再生治療法の開発が進められている．

本稿では，著者らが開発し，既に臨床応用されている自家細胞による角膜上皮再生治療法と，現在，研究開発中である角膜内皮再生医療について述べる．

1. 角膜上皮の再生医療

角膜上皮は角膜の最表層に存在する厚さ約50 μmの非角化重層扁平上皮である(図1-a)．角膜上皮は，表層細胞のタイトジャンクション形成やムチン産生により外界とのバリア機能を担っている．他の重層扁平上皮と同様，ターンオ

大阪大学大学院医学系研究科 脳神経感覚器外科学(眼科学)

0047-1852/11/¥60/頁/JCOPY

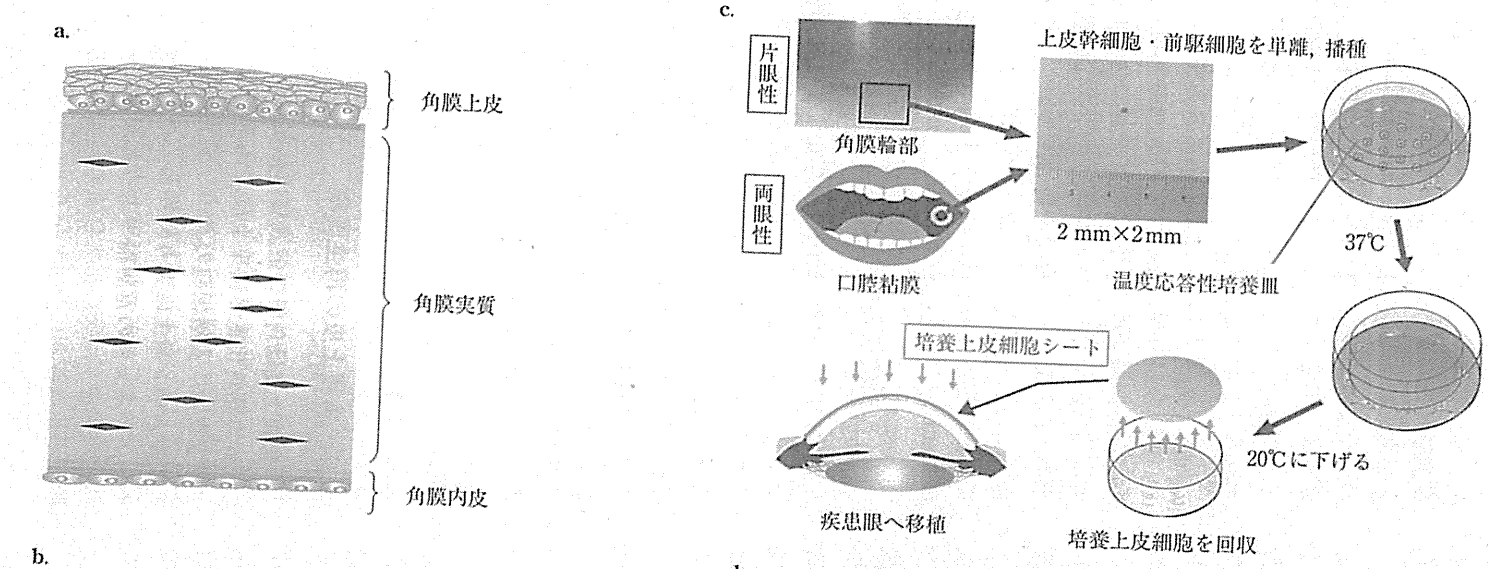

図1　角膜上皮幹細胞と角膜上皮幹細胞疲弊症
(文献[8,9]より引用)

a. 角膜は上皮，実質，内皮の3層からなる．

b. 角膜上皮幹細胞は輪部組織の上皮基底部に局在している．

c. 自家培養上皮細胞シートによる角膜上皮再生治療法の概要．2×2mmの輪部組織(片眼性)あるいは口腔粘膜組織(両眼性)を患者自身から採取→酵素処理で幹細胞・前駆細胞を含む上皮細胞を単離→上皮細胞を温度応答性培養皿上で培養(37℃)→温度を下げて(20℃)培養上皮細胞シートを剥離→疾患眼へ移植．

d. 自家培養上皮細胞シート移植による臨床成績．培養上皮細胞シート移植術前後の眼表面像(左：術前，右：術後)．

ーバーが激しく，1週間ほどで入れ替わるといわれている．この角膜上皮細胞を供給する角膜上皮幹細胞は，角膜と結膜の境界に位置する輪部と呼ばれる組織の上皮基底部に存在すると考えられている(図1-b)．角膜上皮幹細胞は，角膜上皮型分化マーカー(ケラチン3，12)を発現せず，p63やN-cadherinなどの幹細胞・前駆細胞マーカーを発現し，また細胞分裂が緩やかであるなどの特性を有している[1-3]．この上皮幹細胞が外傷や疾患によって機能不全となり喪失すると(角膜上皮幹細胞疲弊症)幹細胞からの角膜上皮細胞の供給ができなくなり，角膜混濁などの重篤な視力障害が起きる．これに対して，角膜上皮前駆細胞を含むとされる角膜輪部を用いた他家角膜移植が実施されてきたが，拒絶反応などのため，術後成績は良好でなかった．

この問題に対処するため，まず，片眼性の疾患に対して，健常な角膜輪部(上皮幹細胞を含むと考えられる)をソースとして培養角膜上皮細胞シートを作製し，疾患眼へ移植する方法が開発された[4-7]．この方法では上皮細胞シート移植により完成された組織だけでなく，上皮幹細胞も移植されることにより，角膜上皮の恒常性が保たれる．これにより角膜上皮疾患に対して再生医療的アプローチによる治療の道が開かれた．しかしながら，臨床的には角膜上皮幹細胞疲弊症は両眼性のものが多く，また，両眼性の方が患者QOLの低下は当然著しい．この場合は，健常な角膜輪部をソースとして使用できないため，新たな幹細胞供給源が必要であった．

著者らはこの問題を解決すべく幹細胞供給源として，口腔粘膜細胞を使用し細胞シートを作製した．このシートは*in vivo*角膜と同様に重層化しており，基底部には上皮幹細胞・前駆細胞が保持されている．更に著者らはこれに，温度応答性培養皿の技術を組み合わせ，移植に使用でき，基質や酵素処理を必要としない独自の自家培養上皮細胞シート移植法を世界に先駆けて開発した[8](図1-c)．片眼性疾患の場合には，健常眼の輪部上皮，両眼性疾患の場合では口腔粘膜上皮より上皮幹細胞・前駆細胞を単離し，温度応答性培養皿上で培養する．この温度応答性培養皿は，37℃では培養皿表面が疎水性となるため細胞が接着するが，32℃以下では，相転移により表面が親水性となり細胞が接着できない．このため，この培養皿上で培養した細胞は酵素処理を必要とせず，温度を下げるという極めて非侵襲的な方法により，細胞接着装置を保持したまま培養上皮細胞シートを回収することが可能である．これにより，基底面の細胞接着分子が保持されているため，移植後に短時間で無縫合でも眼表面に接着することが可能となり，羊膜やフィブリンゲルなどの基質を必要としない．著者らは世界に先駆けてStevens-Johnson症候群，眼類天疱瘡，化学腐食などの角膜上皮幹細胞疲弊症患者に対して，この自家口腔粘膜培養上皮細胞シート移植を行い，良好な成績を得ることに成功している[9](図1-d)．現在は，この治療を本疾患の標準治療とすべく，多施設臨床試験を計画している．

2. 角膜内皮の再生

角膜内皮は角膜の最内層に存在する単層の組織であり，実質側から前房内に水を能動輸送する機能(ポンプ機能)およびバリア機能により，実質内の含水率を一定に維持し，角膜の透明性を維持している(図1-a)．この機能が低下した場合，角膜実質および上皮の含水率が上昇し，透明性が維持されず，角膜が混濁し視力は大きく低下する水疱性角膜症と呼ばれる病態となる．また，ヒト角膜内皮細胞は一度障害を受けると，基本的に再生せず，不可逆的に角膜内皮細胞数が減少してしまう．このような状態は，先天性，加齢，手術による影響などで比較的容易に起こり，この減少が大きい場合水疱性角膜症となる．この状態に対して，以前はドナーの角膜全層を移植することが行われていたが，近年，ドナー角膜の内層(実質の一部と内皮)を移植するパーツ移植が行われるようになり，視力予後の改善に貢献している．しかしながら，ドナー角膜が必要であることには変わりがなく，むしろ，術式改良に伴う適応の拡大により，よりドナー角膜の不足は深刻になっているといえる．

この問題に対処するため，著者らは培養細胞

シート移植技術を用いた角膜内皮再生治療法の開発を行っている(図2-a). ヒト角膜内皮細胞は*in vivo*では増殖しないが, *in vitro*ではある程度, 増殖することが知られている. 著者らはこれまでに, 研究用輸入アイバンク角膜より採取したヒト角膜内皮を温度応答性培養皿上で培養することで, ヒト培養角膜内皮細胞シートを作製, 回収することに成功している(図2-b). 回収した培養角膜内皮細胞シートは, *in vivo*角膜内皮同様の機能を有しており, 更に家兎水疱性角膜症モデルへの移植により, 角膜厚および角膜透明性の有意な改善を認めている[10](図2-c). この方法を用いて角膜内皮細胞をある程度増幅することは可能であるが, 1つのドナー角膜から多数の培養角膜内皮細胞シートを作製することは現時点では困難である. つまり, 現在の技術では1つの献眼から多数の移植シートは作れず, ドナー不足の解決にはつながらない.

一方で, 拒絶反応の問題を完全に克服するために, 自家細胞源を用いた角膜内皮再生治療法の開発が必要である. そのためには, 自家細胞源として角膜内皮疾患の患者自身の角膜内皮細胞を採取することは不可能であるため, 角膜内皮以外の(幹)細胞源を探索することが急務である. これまでに著者らは, 成体の虹彩実質中に角膜内皮と同様に神経堤より由来し, 多分化能を有する細胞が存在することを見いだしている[11]. この虹彩実質中に存在する多能性の組織幹細胞を用いて, 角膜内皮細胞へ分化誘導あるいは再プログラムすることが可能であれば, 自家移植も可能になると考えられ, 現在更に詳細な解析を行っている.

3. 角膜再生医療の今後

著者らは再生医学に基づいた角膜再生治療法の開発に取り組んできた. 角膜上皮再生医療については, 世界に先駆けて温度応答性培養皿を用いた自家の培養上皮細胞シート移植法の臨床応用に成功し, 拒絶反応とドナー不足という2つの問題を同時にクリアすることが可能となり, 今後は標準医療として確立していくことが重要となっている. しかしながら, 解明すべき課題はまだある. 角膜上皮再生医療においては完成された角膜上皮組織を移植するだけでは不十分で, 角膜上皮幹細胞を同時に移植し, 維持しなくてはならない. 現在, 実験レベルでは幹細胞が長期に移植角膜に認められること, 臨床的にも長期成績が良好なことより, 幹細胞が維持されているのはほぼ確実であるが, その詳細な機構については現在も不明のままである. 著者らは移植された上皮細胞シートが均一に幹細胞を含んでいるのではなく, 部位によって含まれる幹細胞やその増殖能に差があることを突き止めている. 今後は, その詳細な機構メカニズムを解明し, より長期に安定で良好な幹細胞の維持を目指すべきである.

内皮細胞は完成された組織を移植することができれば, 幹細胞を移植, 維持しなくても病態を改善することができる分, ハードルは低く思われるが, 現実には上皮に比べ, 再生医療の応用は遅れているといえる. その原因の一つとして, 角膜上皮の場合とは異なり, ヒト角膜内皮細胞, 内皮幹細胞・前駆細胞の特性, あるいは, 幹細胞・前駆細胞についてはその存在自体ですら不明であることが挙げられる. 例えば, 信頼性の高い内皮細胞マーカーもない状態である. そのため, 現在, 角膜内皮細胞・幹細胞・前駆細胞の存在を検証し, それらを増幅・分化させるための様々なアプローチを試みているのが現状である.

また, 日本が誇るべき再生医療の技術はいうまでもなくiPS細胞である. 著者らもまた, iPS細胞から角膜上皮, 内皮への分化誘導法の開発, また, それを用いた移植用の細胞シートの開発を鋭意行っている. この技術が完成すれば, ドナー不足と拒絶反応の問題を一気に解決することができる. このiPS細胞を利用した再生医療を我が国発の世界標準治療として確立し, 一人でも多くの患者に光を届けることが我々の使命と考えている.

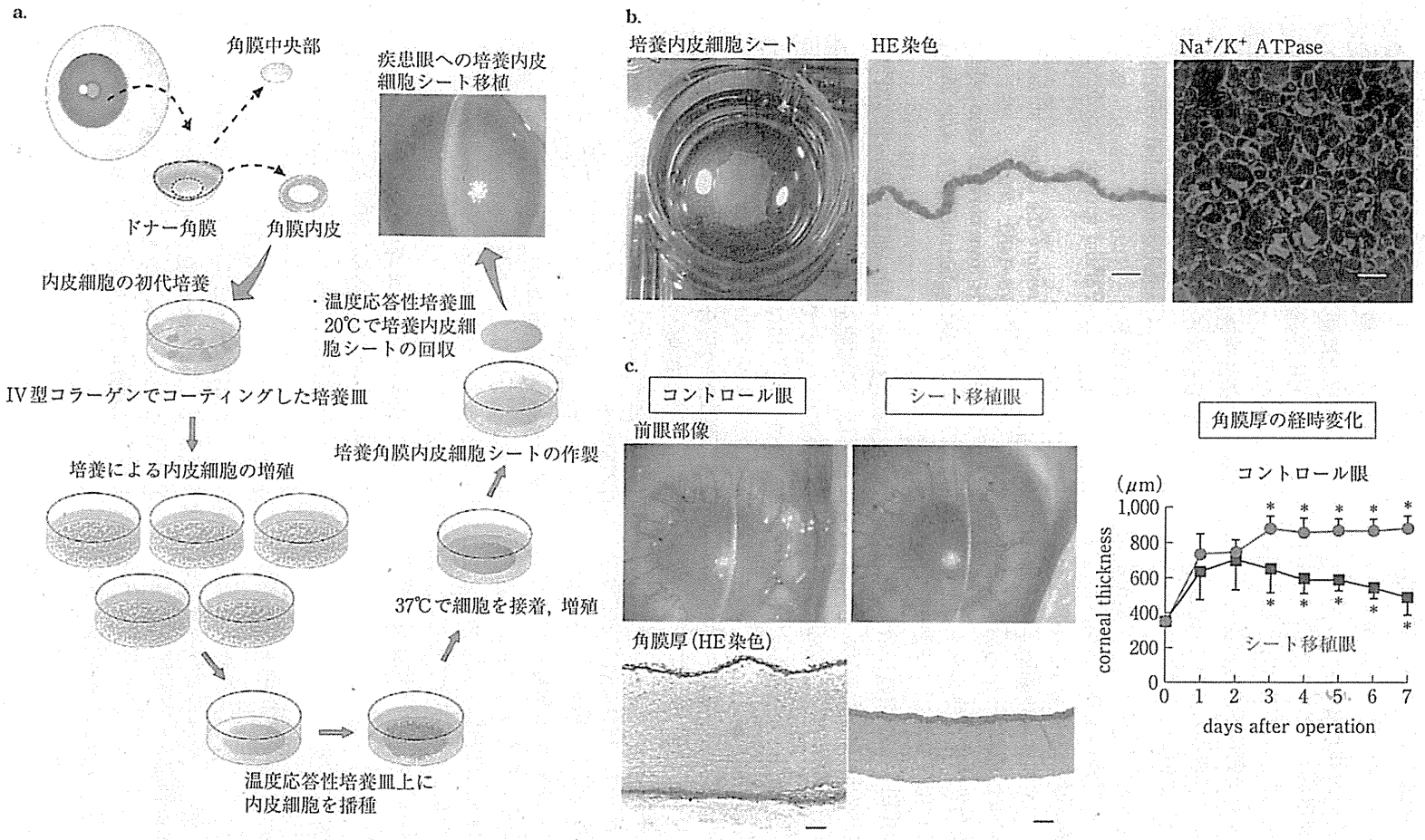

図2　培養角膜内皮細胞シート移植法の概要(文献[10]より引用)

a. 輸入アイバンク角膜の周辺部より角膜内皮を採取→IV型コラーゲンコーティング培養皿上で初代培養→細胞継代により細胞数を増幅→生体と同密度で温度応答性培養皿に播種，37℃で培養→20℃に温度を下げて培養角膜内皮細胞シートを回収→疾患眼へ移植．

b. 温度応答性培養皿より回収した培養角膜内皮細胞シートのHE染色像およびNa^+/K^+ ATPaseの免疫染色．回収した培養角膜内皮細胞シートは*in vivo*角膜内皮組織同様に単層構造を呈し，ポンプ機能を担うNa^+/K^+ ATPaseの発現も認められた(Bar: 20 μm)．

c. 家兎水疱性角膜症モデルへの培養角膜内皮細胞シート移植後の眼表面観察像およびHE染色像．非移植眼に比較して移植眼では角膜透明性と角膜厚の改善が認められた．また経時的な角膜厚測定の結果，移植後3日以降で統計学的に有意な角膜厚の改善が認められた(グラフ)．

圖文 献

1) Schermer A, et al: Differentiation-related expression of a major 64K corneal keratin in vivo and in culture suggests limbal location of corneal epithelial stem cells. J Cell Biol **103**: 49-62, 1986.
2) Cotsarelis G, et al: Existence of slow-cycling limbal epithelial basal cells that can be preferentially stimulated to proliferate: Implications on epithelial stem cells. Cell **57**: 201-209, 1989.
3) Hayashi R, et al: N-Cadherin is expressed by putative stem/progenitor cells and melanocytes in the human limbal epithelial stem cell niche. Stem Cells **25**(2): 289-296, 2007.
4) Pellegrini G, et al: Long-term restoration of damaged corneal surfaces with autologous cultivated corneal epithelium. Lancet **349**: 990-993, 1997.
5) Tsai RJ, et al: Reconstruction of damaged corneas by transplantation of autologous limbal cells. N Engl J Med **343**: 86-93, 2000.
6) Koizumi N, et al: Cultivated corneal epithelial stem cell transplantation in ocular surface disorders. Ophthalmology **108**: 1569-1574, 2001.
7) Rama P, et al: Autologous fibrin-cultured limbal stem cells permanently restore the corneal surface of patients with total limbal stem cell deficiency. Transplantation **72**: 1478-1485, 2001.
8) Nishida K, et al: Functional bioengineered corneal epithelial sheet grafts from corneal stem cells expanded ex vivo on a temperature-responsive cell culture surface. Transplantation **77**: 379-385, 2004.
9) Nishida K, et al: Corneal reconstruction using tissue-engineered cell sheets comprising autologous oral mucosal epithelium. N Engl J Med **351**: 1187-1196, 2004.
10) Sumide T, et al: Functional human corneal endothelial cell sheets harvested from temperature-responsive culture surfaces. FASEB J **20**(2): 392-394, 2006.
11) Kikuchi M, et al: Neural crest-derived multipotent cells in the adult mouse iris stroma. Genes Cells **16**(3): 273-281, 2011.

JCS ePress online publication date 21 February 2012

Chronic photo-oxidative stress and subsequent MCP-1 activation as causative factors for age-related macular degeneration

Mihoko Suzuki[1], Motokazu Tsujikawa[1], Hiroyuki Itabe[2], Zhao-Jiang Du[1], Ping Xie[1], Nagakazu Matsumura[1], Xiaoming Fu[3], Renliang Zhang[3], Koh-hei Sonoda[4], Kensuke Egashira[5], Stanley L. Hazen[3], Motohiro Kamei[1]

1. Department of Ophthalmology, Osaka University Graduate School of Medicine, 2-2 Yamadaoka, Suita, Osaka 565-0871 JAPAN

2. Department of Biological Chemistry, School of Pharmaceutical Sciences, Showa University, 1-5-8 Hatanodai, Shinagawa-ku, Tokyo 142-8555, JAPAN

3. The Center for Cardiovascular Diagnostics and Prevention, Cleveland Clinic, Cleveland Ohio USA. NE10 9500 Euclid Avenue NE10, Cleveland, Ohio, USA 44195

4. Department of Ophthalmology, Yamaguchi University Graduate School of Medicine, 1-1-1 Minami Kogushi, Ube, Yamaguchi 755-8505, JAPAN

5. Department of Cardiovascular Medicine, Graduate School of Medical Sciences, Kyushu University, 3-1-1 Maidashi, Higashi-Ku, Fukuoka 812-8582, JAPAN

Corresponding author
Motohiro Kamei, MD, PhD
Department of Ophthalmology
Osaka University Graduate School of Medicine
2-2 Yamadaoka, #E7, Suita, Osaka 565-0871, JAPAN
Tel: +81-6-6879-3456
Fax: +81-6-6879-3458
e-mail:mkamei@ophthal.med.osaka-u.ac.jp

Abbreviations: AMD, age-related macular degeneration; CNV, choroidal neovascularization; MCP-1, monocyte chemoattractant protein-1; RPE, retinal pigment epithelium; ON-PC (oxidized phospholipids), 9-oxononanoic acid esters of 2-lyso-phosphatidylcholine; PL-PC (non-oxidized phospholipids), 1-palmitoyl-2-linoleoyl-sn-glycero-3-phosphatidylcholine; Ccr2, C-C chemokine receptor2; PBN, α-phenyl-N-tert-butylnitrone; VEGF, vascular endothelial growth factor; PEDF, pigment epithelium-derived factor; Cx3cr1, C-X3-C chemokine receptor 1

Summary

Age-related macular degeneration (AMD) is the leading cause of blindness among the elderly in developed countries. Although pathogenic factors, such as oxidative stress, inflammation, and genetics are thought to contribute to the development of AMD, little is known about the relationships and priorities between these factors. Here, we show that chronic photo-oxidative stress is an environmental factor involved in AMD pathogenesis. We first demonstrated that light exposure induced phospholipid oxidation in the mouse retina, which was more prominent in aged animals. The induced oxidized phospholipids led to an increase in the expression of monocyte chemoattractant protein-1, which then resulted in macrophage accumulation, an inflammatory process. Antioxidant treatment prevented light-induced phospholipid oxidation and the subsequent increase of monocyte chemoattractant protein-1, which are the beginnings of the light-induced changes. Subretinal application of oxidized phospholipids induced choroidal neovascularization, a characteristic feature of wet-type AMD, which was inhibited by blocking monocyte chemoattractant protein-1. These findings strongly suggest that a sequential cascade from photic stress to inflammatory processes via phospholipid oxidation has an important role in AMD pathogenesis. Finally, we succeeded in mimicking human AMD in mice with low level, long-term photic stress, in which characteristic pathological changes, including choroidal neovascularization formation, were observed. Therefore, we propose a consecutive pathogenic pathway involving photic stress, oxidation of phospholipids, and chronic inflammation, leading to angiogenesis. These findings add to the current understanding of AMD pathology and suggest protection from oxidative stress or suppression of the subsequent inflammation as new potential therapeutic targets for AMD.

Introduction

Age-related macular degeneration (AMD) is the leading cause of blindness among the elderly in developed countries (Beatty et al., 2000). AMD is a progressive, polygenic, and multifactorial disease with a poorly understood etiology, although numerous studies have suggested the involvement of factors such as oxidative stress, inflammation, immune response, and genetics in the onset of AMD (Baba et al., 2010; Edwards et al., 2005; Grossniklaus et al., 2002; Haines et al., 2005; Klein et al., 2005; Yates et al., 2007).

Some age-related diseases may have pathologically common molecular mechanisms, and we focused on the histopathologic similarities between AMD and atherosclerosis. We previously demonstrated that photoreceptor phospholipids in the macula are more oxidized in eyes with AMD than in age-matched normal eyes (Suzuki et al., 2007) and that accumulated macrophages in AMD lesions express scavenger receptors for oxidized phospholipids (Kamei et al., 2007). Other studies analyzing human eyes with AMD also suggest the involvement of lipid uptake (Malek et al., 2003) and an immune response to oxidized lipids produced by oxidative stress (Hollyfield et al., 2008). Oxidized phospholipids stimulate the expression of vascular endothelial growth factor(VEGF) (Bochkov et al., 2006), which induces inflammatory gene expression (Furnkranz et al., 2005) as well as neovascularization. The detailed mechanisms underlying the involvement of oxidized phospholipids in AMD, however, remain unknown. Therefore, in the present study, we examined the molecular mechanisms underlying the involvement of oxidized phospholipids in AMD pathogenesis and compared them with the pathogenic mechanisms of atherosclerosis.

AMD affects the macula, the center area of the retina, where light is focused throughout life. We hypothesized that light causes oxidative stress to the macula. Although there are numerous reports that intensive light irradiation causes retinal damage, known as phototoxicity, we evaluated low-intensity, long-term, light exposure as an enhanced model of the effects of light in daily life.

In this paper, we propose a pathogenic pathway from light exposure to choroidal neovascularization (CNV) formation, a characteristic feature of AMD, involving oxidative stress and chronic inflammation.

Results

Light induces phospholipid oxidation in the retina.

We first investigated whether subacute mid-level light exposure (1000 lux for 1 week, Fig. 1A) induces lipid oxidation in the retina. After light exposure in the mouse retina, mass spectrometry analyses revealed a significant increase in 9-oxononanoic acid esters of 2-lyso-phosphatidylcholine (ON-PC; $p<0.001$), 4,7-dioxohept-6-enoic acid esters of 2-lyso-phosphatidylcholine (KOHA-PC; $p=0.037$), and succinic acid esters of 2-lyso-phosphatidylcholine (S-PC; $p=0.006$), and no changes in azeleic acid esters of 2-lyso-phosphatidylcholine (A-PC; $p=0.642$), 4-hydroxy-7-oxohept-5-enoic acid esters of 2-lyso-phosphatidylcholine (HOHA-PC; $p=0.533$) and 4-oxobutyric acid esters of 2-lyso-phosphatidylcholine (OB-PC; $p=0.812$; Fig. 1B). Therefore, ON-PC was used as a representative oxidized phospholipid. Oxidized phospholipids were observed in the retinas of untreated normal animals (Fig. 1C,E), but seemed more prominent in aged animals (Fig. 1E), and their distribution involved the entire sensory retina from the nerve fiber layer to the photoreceptor outer segments, the retinal pigment epithelium (RPE), and the choroid. Light irradiation increased immunostaining for oxidized phospholipids in the retinas of both 2-month-old and 12-month-old mice (Fig. 1D,F). Oxidized phospholipids in the outer plexiform layer, the photoreceptor outer segments, RPE, and the choroid were more prominent in the older mice (Fig. 1F) compared with the younger mice (Fig. 1D). A competitive enzyme-linked immunosorbent assay (competitive ELISA) revealed a significant increase in oxidized phospholipids in the retinas of irradiated mice compared with non-irradiated mice in both 2-month-old and 12-month-old mice ($p<0.001$; Fig. 1G). Irradiated older mice had significantly more oxidized phospholipids than irradiated younger mice ($p=0.003$). Although the sleep duration of irradiated mice was not monitored closely, there was no obvious interruption of normal sleep patterns because they didn't show any weight loss, epilation, abnormal behavior, or early mortality compared with control mice. Thus, photic stress induced phospholipid oxidation in the retina, and older animals were more susceptible to photic stress than younger animals.

Oxidized phospholipids induce monocyte chemoattractant protein-1 (MCP-1) in RPE cells and light irradiation elicits MCP-1 in the retina in vivo.

We next investigated reactions induced by phospholipid oxidation in the retina. We examined

whether oxidized phospholipids induce MCP-1 (also known as CCL2), an important chemotactic factor for macrophages (Lu et al., 1998), which have a key role in human AMD (Grossniklaus et al., 2002). Both oxidized phospholipids (ON-PC) and non-oxidized phospholipids (1-palmitoyl-2-linoleoyl-*sn*-glycero-3-phosphatidylcholine [PL-PC]), increased the amount of MCP-1 protein released by RPE cells in a dose-dependent manner. RPE cells released more MCP-1 following treatment with oxidized phospholipids compared with non-oxidized phospholipids (concentrations up to 50 μg/ml, Fig. 2A). In the in vivo analysis, MCP-1 mRNA and protein significantly increased after light irradiation in both 2-month-old and 12-month-old mice ($p<0.001$; Fig. 2B,C). The increase was more evident in older mice. MCP-1 immunostaining in the RPE was notable in the retinas of light-irradiated 12-month-old mice, whereas there was no apparent staining in non-irradiated retinas (Fig. 2D). Macrophages accumulated in the choroid of the 12-month-old mice after long-term low-intensity light irradiation (500 lux for 2 months; Fig. 2E). These findings suggest that photo-oxidative stress induces the expression of MCP-1 via the oxidation of phospholipids, which have an important role in inducing inflammation, especially in older animals.

Oxidized phospholipids induce CNV.

To confirm that the cascade subsequent to photo-oxidative stress has an important role in AMD development, oxidized phospholipids (ON-PC) or non-oxidized phospholipids (PL-PC) were injected into the subretinal space of wild-type mice. Although CNV was not observed in the control eyes injected with non-oxidized phospholipids (Fig. 3A), all eyes receiving oxidized phospholipids exhibited apparent CNV formation within 4 weeks following the subretinal injection (Fig. 3B).

Oxidized phospholipids induce CNV in wild-type retinas but not in CCR2$^{-/-}$ and MCP-1$^{-/-}$ mice.

We then injected oxidized phospholipids into the subretinal space of two different knockout (KO) mouse lines, MCP-1$^{-/-}$ and CCR2$^{-/-}$ (MCP-1 receptor KO), to examine the involvement of the MCP-1 pathway in CNV formation. CNV did not develop after subretinal injections of oxidized phospholipids into MCP-1$^{-/-}$ mice (Fig. 3D) or CCR2$^{-/-}$ mice (Fig. 3F), whereas CNV developed in the eyes of their wild-type siblings (Fig. 3B). CNV was not observed in any eyes

injected with non-oxidized phospholipids (Fig. 3A,C,E). These results indicated that activation of the MCP-1 pathway by oxidized phospholipids has a pivotal role in CNV formation in vivo.

Long-term, low-intensity photo-oxidative stress induces basal laminar deposits, macrophage accumulation, and CNV formation.

The results of the above experiments confirmed that the cascade from photic stress to MCP-1 activation via phospholipid oxidation in the retina could have a pivotal role in CNV formation in vivo. We, therefore, attempted to mimic human AMD in mice using long-term, low-level light irradiation. Basal laminar deposits, an essential histopathologic feature of AMD, were observed in the eyes of animals exposed to low-level blue-light irradiation (500 lux) every 2 days for 4 to 6 months (Fig. 4A). Subsequently, in 4 of 8 eyes, CNV was observed by fundus examination (Fig. 4B). Fluorescein angiography revealed that the CNV was the occult-dominant type (Fig. 4C), the major CNV type observed in human AMD, and typical histopathologic features of CNV in human AMD, including a thickened and proliferated vascular lesion between the RPE and Bruch's membrane (Fig. 4D). Electron microscopic and immunohistochemical examinations showed that macrophages accumulated around the CNV and engulfed the photoreceptor outer segments, including the oxidized phospholipids (Fig. 4E), as observed in human CNV lesions (Lu et al., 1998). The lack of CNV in both MCP-$1^{-/-}$ (n=4) and $CCR2^{-/-}$ mice (n=6) under the same irradiating conditions confirmed that the MCP-1 pathway is key in CNV development induced by long-term low-intensity light irradiation (Fig. 4F).

Prevention of oxidative changes and monocyte chemoattractant protein-1 (MCP-1) induction by α-phenyl-N-tert-butylnitrone (PBN).

To confirm that oxidative stress itself is the cause of light-induced changes, α-phenyl-N-tert-butylnitrone (PBN), an antioxidant, was daily injected intraperitoneally to 12-month-old mice during light irradiation (1000 lux for 1 week). PBN (Fig. 5C) suppressed the increased immunostaining for oxidized phospholipids after light irradiation (Fig. 5A, B). The light-induced increases of MCP-1 immunoreactivity (Fig. 5D, E), mRNA (Fig. 5G), and protein (Fig. 5H) were significantly suppressed by the PBN treatment ($p<0.05$; Fig. 5F,G,H).

VEGF expression in the light-induced CNV and decrease of VEGF expression by MCP-1

siRNA treatment in RPE cells

To investigate whether VEGF, a major angiogenic cytokine, and PEDF, a potent angiogenic inhibitor, are involved in CNV formation by long-term, low-intensity light exposure, the expression of VEGF and PEDF were examined in light-induced CNV. Strong VEGF immunoreactivity was detected in light-induced CNV lesions (Fig. 6A), where strong VEGFR2 immunoreactivity was also detected (Fig. 6B). PEDF immunoreactivity was weak in light-induced CNV lesions (Fig. 6C). Next, we examined whether or not RPE-derived MCP-1 mediates the expression of VEGF and PEDF. RPE cells released VEGF with both oxidized and non-oxidized phospholipids in a dose-dependent manner, and more VEGF was released following treatment with oxidized phospholipids than with non-oxidized phospholipids (concentrations 10, 25 and 50 μg/ml, $p<0.001$) (Fig. 6D). These elevated VEGF levels were significantly decreased by MCP-1 siRNA treatment ($p<0.05$, $n=6$; Fig. 6D). PEDF protein levels did not differ significantly in RPE cells treated with either oxidized or non-oxidized phospholipids (concentrations 10, 25, and 50 μg/ml). MCP-1 siRNA treatment did not affect PEDF production following treatments with either oxidized or non-oxidized phospholipids (Fig. 6E).

Discussion

The development of an AMD animal model following long-term, low intensity light exposure in the present study suggests that light exposure is an environmental factor that contributes to AMD pathogenesis. Light exposure inevitably causes oxidative stress to the retina, especially in modern life, as we are surrounded by artificial lights such as indoor illumination, computer monitors, and television. Some epidemiological studies suggest that light exposure is linked to AMD (Cruickshanks et al., 1993; Taylor et al., 1992), while others do not (Clemons et al., 2005). Even the study finding no apparent link between light exposure and AMD development, however, reported that low levels of dietary antioxidants, including lutein and vitamin C, are associated with an increased risk for AMD, which is supported by other studies (Age-Related Eye Disease Study Research Group et al., 2007; Tan et al., 2008; van Leeuwen et al., 2005).

The present findings demonstrated that blue light exposure induces oxidative stress and chronic inflammation, which are more prominent in aged animals. These effects seem to be due to light directly and not to the interruption of normal sleep patterns by continuous irradiation

because the mice in the experiments appeared to have normal sleep/wake patterns. In addition, these changes are suppressed by an antioxidant. This suggests that AMD is more likely to develop in persons who are more susceptible to oxidative stress due to decreased antioxidant activity or in persons who have an exaggerated immune response to oxidized products. Our results also demonstrate that elevated VEGF expression by oxidized phospholipids in RPE cells is suppressed by MCP-1 siRNA. Therapeutic strategies to protect phospholipids from photic stress-induced oxidation or to suppress the subsequent inflammation induced by biologically active lipid peroxidation products warrant further investigation.

The present study suggests that photic stress induces MCP-1 via the oxidation of phospholipids in the retina, which may have an important role in inducing inflammation in AMD pathogenesis. The mechanism of the oxidized phospholipid-mediated inflammatory response plays an important role in other age-related diseases, including atherosclerosis (Bochkov et al., 2006), where MCP-1 plays a key pathogenic role. In the current study, MCP-1or its cognate Ccr-2 KO mice did not show obviously cardinal features of AMD, including drusen, which are deposits of a protein/lipid complex, photoreceptor atrophy and CNV, as previously reported (Ambati et al. 2003), although in both wild-type and MCP-1 or Ccr-2 KO mice, the white spots increased with age at the same level. The role of MCP-1 in AMD pathogenesis is controversial; some research groups reported that downregulation of MCP-1 suppressed CNV formation (Yamada et al., 2007), while others showed the AMD-like phenotype in Ccl-2 (identical to MCP-1) KO mice (Ambati et al., 2003). The former demonstrated that the downregulation of MCP-1 decreased CNV size via reduction of macrophage infiltration, while the latter showed that MCP-1 deficiency caused less macrophage accumulation and allowed accumulation of C5a and IgG, which induces VEGF production by RPE and provides an environment permissive for CNV. Ccl-2/Cx3cr1-deficient mice with aberrant MCP-1 signaling show retinal angiomatous proliferation, a type of CNV in AMD (Zhou et al., 2011). Considering these previous reports and our current study together, we speculate that MCP-1 impairment can serve both pro-and anti-angiogenesis roles depending on the circumstances.

The findings of the present study make a significant contribution to AMD research by providing an animal model that mimics the human disease. Mimicking human CNV in model animals has been difficult to date. Laser-induced CNV is currently the only widely used model. The CNV in the laser-induced model, however, is pathologically different from human CNV

because it produces a granuloma resulting from the trauma induced by a laser intense enough to rupture Bruch's membrane located between the RPE and choroid, and represents only classic CNV, which is not a major type of CNV such as occult-dominant CNV in humans. Although the CNV model in this study requires aged animals and several months of light exposure, it more closely resembles the human pathology compared to the laser-induced CNV animal models, which will significantly advance the development of novel treatments for AMD.

Materials and methods

Animals

MCP-1$^{-/-}$ mice backcrossed to a C57BL/6 background were purchased from Jackson Laboratory (Bar Harbor, ME). Ccr2$^{-/-}$ mice with a 129xB6 background were generated as described previously (Boring et al., 1997). Littermates were used as controls in each experiment. All experiments were performed in accordance with the Association for Research in Vision and Ophthalmology Statement for the Use of Animals in Ophthalmic and Vision Research.

Light exposure

Freely moving 2-month-old and 12-month-old C57BL/6 male mice were exposed to a blue light-emitting diode (LED) continuously for 1 week (Moritex, Tokyo, Japan; illuminance: 1000 lux, transmission peak wavelength: 480 nm). For low-level light irradiation, freely moving 6-month-old wild-type, MCP-1$^{-/-}$, and Ccr2$^{-/-}$ mice were exposed to a blue LED every 2 days for 6 months (Moritex; illuminance: 500 lux, transmission peak wavelength: 480 nm, Fig. 1A). They were maintained on a 12-hour:12-hour light-dark cycle with dim overhead fluorescent light in the whole room.

Mass spectrometric analysis of phospholipids

Lipid extracts were re-dissolved in methanol:water (90:10) and liquid chromatography/electrospray ionization tandem mass spectrometry (LC/ESI/MS/MS) performed using a Prodigy ODS C18 column for separation of the lipids and the HPLC solvent system (Waters, Milford, MA). Mass spectrometric analyses were performed using ESI/MS/MS in the positive ion, multiple reaction monitoring (MRM) mode (cone energy 30 V/collision energy 25 eV). The MRM transitions used to detect individual oxidized phospholipids were the mass to

charge ratio (*m/z*) for the molecular cation $[M+H]^+$ and their daughter ion 184, the phosphatidylcholine group. Calibration curves for quantitative analyses of individual oxidized phosphatidylcholine molecular species were constructed by mixing a fixed amount of internal standard (ditetradecyl phosphatidylcholine) into various amounts of authentic oxidized phosphatidylcholine samples (Sun et al., 2006).

Immunohistochemistry

Enucleated mouse eyes were immersed in ice-cold phosphate-buffered 4% paraformaldehyde for 6 hours. Eyes were infiltrated with 30% sucrose and embedded in OCT compound (Sakura Finetechnical Co., Tokyo, Japan). Sections (8 μm) were cut, air-dried for 3 hours, and stored at -80°C. Immunofluorescent staining was performed using standard protocols with digitonin permeabilization. Briefly, sections blocked with 5% normal donkey serum were incubated overnight at 4°C with mouse monoclonal antibody to human oxidized phosphatidylcholine, DLH3 (1:100, provided by Dr. Hiroyuki Itabe (1994)), goat polyclonal antibody to mouse MCP-1 (1:100, R&D Systems, Minneapolis, MN), rat monoclonal antibody to F4/80 (1:100, Serotec), rabbit polyclonal antibody to mouse PEDF (1:100, Santa Cruz Biotechnology, Inc., Santa Cruz, CA) , rabbit polyclonal antibody to mouse VEGF or VEGFR2 (1:100, Abcam, Cambridge, MA) . Slides were washed three times with Tris-buffered saline containing 0.1% Tween 20 and incubated with Alexa Fluor 546–conjugated secondary antibodies or Alexa Fluor 488–conjugated secondary antibodies (Invitrogen, Carlsbad, CA) for 60 min at room temperature.

Competitive ELISA for oxidized phospholipids

Relative amounts of oxidized phospholipids in the retinas were evaluated using a competitive ELISA as described in a previous report (Itabe et al., 1994), which is a modified sandwich ELISA procedure for determining oxidized low density lipoprotein (OxLDL). Briefly, microtiter wells precoated with the monoclonal antibody, DLH3 (5 μg/ml in phosphate-buffered saline [PBS], 100 μl/well) were blocked with 1% bovine serum albumin in 50 mM Tris-buffered saline, pH 8.0. One hundred microliters of a solution of lipids extracted from retinas, which were resuspended in PBS, was placed in each well and left at room temperature for 30 min, followed by the addition of 10 μl OxLDL (1 μg/ml). The OxLDL that remained after washing with Tris-buffered saline containing 0.05% Tween 20 was detected by 100 μl sheep anti-human apoB IgG

(Chemicon, Temecula, CA) and 100 µl alkaline phosphatase-conjugated donkey anti-sheep IgG antibody (Chemicon). Alkaline phosphatase reactivity was measured by incubating 1 mg/ml of p-nitrophenylphosphate at 37°C for the appropriate time intervals. Antigenic activity was expressed as a percentage of inhibition, calculated as (Abs (OxLDL)-Abs (sample + OxLDL)) ×100/ (Abs (OxLDL) - Abs (PBS)).

Lipids

Oxidized phospholipids (ON-PC; 9-oxononanoic acid esters of 2-lyso-phosphatidylcholine [2-lyso-PC]) and phospholipids (PLPC; linoleic acid) were purchased from Avanti Polar Lipids, Inc. (Alabaster, AL)

Cell culture

The human retinal pigment epithelial cell line ARPE-19 was obtained from the American Type Culture Collection and cultured in Dulbecco's modified Eagle's medium/F-12 supplemented with 10% fetal bovine serum, penicillin (100 U/mL), and streptomycin sulfate (100 µg/mL). Cells were grown at 37°C in humidified 5% CO_2 and split twice a week when approximately 90% confluent. Cells were obtained at passage 12 and used at passages 14 to 18. RPE cells were subcultured in 24-well tissue culture plates at a density of $4x10^4$ cells/well. Seven days after reaching confluence, the medium was changed and cells were incubated in serum-free Dulbecco's modified Eagle's medium in the presence or absence of untreated phospholipids or oxidized phospholipids at concentrations of 0, 10, 25, or 50 µg/ml. After 6 h, the medium was collected, filter sterilized, and stored at -80°C until use for ELISA for MCP-1. Each condition was evaluated in triplicate, and results were repeated in at least three independent experiments.

Real-time RT-PCR for MCP-1

For analysis of MCP-1 mRNA levels in the retina-RPE-choroid complex, total RNA was isolated from the respective samples (RNeasy Mini Kit, Qiagen Inc., Valencia, CA) and reverse-transcribed with a cDNA synthesis kit (First-Strand, Amersham Biosciences/GE Lifesciences; Piscataway, NJ). We used β-actin as the invariant control. Commercially available primers and probe sets of the mouse MCP-1 genes (Invitrogen) were prepared for the analysis. We performed amplification, detection, and data analysis using the ABI PRISM 7900 Sequence Detection

System.

ELISA

The retina-RPE-choroid complex was placed into 200 ml of lysis buffer supplemented with protease inhibitors and sonicated. The lysate was centrifuged at 15,000 rpm for 10 min at 4°C. The supernatants and amount of secreted MCP-1,VEGF, or PEDF in the conditioned medium from RPE cells were assayed with ELISA kits for MCP-1,VEGF (R&D Systems) and PEDF (BioVendor, Czech Republic) according to the manufacturer's protocols. Protein concentrations were determined using the BCA protein assay kit (Pierce, Rockford, IL).

Subretinal injection of oxidized phospholipids or non-oxidized phospholipids

Subretinal injections were performed on 8-week old C57BL/6J, $MCP^{-/-}$, and $Ccr2^{-/-}$ mice. The mice received phospholipids (50 μg/ml) in one eye and oxidized phospholipids (50 μg/ml) in the other eye. At this concentration, there was no significant difference in the cell survival of ARPE-19 cells after exposure to oxidized phospholipids and phospholipids. Pulled glass micropipettes were calibrated to deliver 2 μl of vehicle upon depression of a foot switch (FemtoJet Express; Eppendorf). The mice were anesthetized with ketamine hydrochloride (100 mg/kg body weight) and xylazine (10 mg/kg body weight), pupils were dilated with topical 1% tropicamide (Santen Inc., Napa, CA), and the sharpened tip of the micropipette (Eppendorf) was passed through the sclera 1 mm posterior to the limbus and positioned adjacent to the retina. Depression of the foot switch caused the injection fluid to penetrate the retina. Injections were performed using a condensing lens system, which allowed visualization of the retina during the injection. This technique is atraumatic and the direct visualization allows for confirmation of a successful injection by the appearance of a small retinal bleb. All injections were made at a site approximately two-thirds of the distance vertically from the optic disc to the ora serrata in the superior retina.

Histology examination

For histology, the eyes were enucleated and fixed with 4% paraformaldehyde for 1 hour h at 4° . After removing the anterior segment, the eyecups were fixed again in 4% paraformaldehyde overnight, dehydrated in 30% sucrose for 6 hours, and then embedded in Tissue-Tek® OCT

compound. The eyecups were sectioned into 7-μm thick slices and stained with hematoxylin and eosin.

Electron microscopy

The retina-RPE-choroid was fixed in 2.5% glutaraldehyde solution for 2 hours and 1% osmium tetroxide solution for 1 hour, rinsed in PBS, dehydrated in EtOH, and then embedded in epoxy resin (Nissin EM Quetor 812). Thick (1.0 μm) and ultrathin sections (80 nm) were cut on a ultramicrotome (Reichert Ultracut E). The thick sections were stained with toluidine blue and examined by light microscopy. Ultrathin sections were stained with 4% uranyl acetate and lead citrate and then examined with an H-7650 transmission electron microscope (Hitachi, Tokyo, Japan).

Fluorescein Angiography

Fluorescein angiography was recorded using a fundus camera (RC-2, Kowa) with an external 66-diopter condensing lens mounted between the camera and the eye. The pupil was dilated with topical 1% tropicamide (Santen) and mice were injected intraperitoneally with 10% sodium fluorescein (Ak-Fluor) at a dose of 0.03 ml/5 g weight.

PBN Treatment

α-Phenyl-N-tert-butylnitrone (PBN), a commonly used free radical spin trap (Ranchon I., et al. 2003), was purchased from Sigma-Aldrich (St. Louis, MO) and dissolved in saline. PBN (50 mg/kg) was intraperitoneally administered once daily for a week with light irradiation.

MCP-1 siRNA treatment

Transfection of MCP-1 siRNA (Santa Cruz Biotechnology, Inc.) was performed according to the manufacturer's instructions. ARPE-19 cells treated with MCP-1 siRNA were incubated in serum-free Dulbecco's modified Eagle's medium in the presence or absence of untreated phospholipids or oxidized phospholipids at concentrations of 0, 10, 25, or 50 μg/ml. After 6 h, the medium was collected, filter sterilized, and stored at -80°C until use for ELISA for VEGF or PEDF. Each condition was evaluated in triplicate, and the results were repeated in at least three independent experiments.